Negative ion production in collisions between K(n d) Rydberg atoms and CF3Br and CF2Br2

A. Kalamarides, R. W. Marawar, X. Ling, C. W. Walter, B. G. Lindsay, K. A. Smith, and F. B. Dunning

Citation: The Journal of Chemical Physics **92**, 1672 (1990); doi: 10.1063/1.458048
View online: http://dx.doi.org/10.1063/1.458048
View Table of Contents: http://scitation.aip.org/content/aip/journal/jcp/92/3?ver=pdfcov
Published by the AIP Publishing

Negative ion production in collisions between K(*nd*) Rydberg atoms and CF_3Br and CF_2Br_2

A. Kalamarides, R. W. Marawar, X. Ling, C. W. Walter, B. G. Lindsay, K. A. Smith, and F. B. Dunning

Department of Space Physics and Astronomy and the Rice Quantum Institute, Rice University, Houston, Texas 77251

(Received 27 July 1989; accepted 25 October 1989)

Negative ion production via electron transfer in collisions between K(*nd*) Rydberg atoms and CF_3Br and CF_2Br_2 has been investigated over a wide range of of n ($10 \lesssim n \lesssim 70$). For both species, the major negative ion observed is Br^-, although with CF_2Br_2, a small Br_2^- signal is also detected. Kinematic studies show that Br^- production via dissociative attachment is accompanied by sizable translational energy release (~ 0.35 eV for CF_3Br; ~ 0.2 eV for CF_2Br_2). These studies further show that, despite this large energy release, post-attachment interactions between the product ions are important at intermediate values of n ($n \lesssim 20$) and suggest that the transient CF_3Br^{-*} and $CF_2Br_2^{-*}$ ions initially formed by electron capture have quite different lifetimes against dissociation. Cross sections for free-electron attachment to both species are derived from measurements of rate constants for electron transfer at high n. These cross sections are in reasonable agreement with results obtained in free-electron studies using the threshold photoelectron spectroscopy technique.

INTRODUCTION

A study of negative ion production in collisions between potassium atoms in high-lying *nd* states and CF_3Br and CF_2Br_2 via the electron transfer reactions

$$K(nd) + CF_3Br \rightarrow K^+ + CF_3Br^{-*} \rightarrow CF_3 + Br^-, \quad (1)$$

$$K(nd) + CF_2Br_2 \rightarrow K^+ + CF_2Br_2^{-*} \rightarrow CF_2Br + Br^- \quad (2a)$$

$$\rightarrow CF_2 + Br_2^- \quad (2b)$$

is reported. For large values of principal quantum number n, such collisions can be described by the essentially free electron model.[1] This model assumes that the separation between the excited Rydberg electron and its associated core ion is so large that negative ion production can be discussed simply in terms of capture of the Rydberg electron by the target molecule. Because the mean kinetic energy of the Rydberg electron is low ($\sim 13.6/n^2$ eV), Rydberg atom studies provide a novel means to explore electron–molecule interactions at subthermal electron energies.[2]

In the present work, rate constants for negative ion production via reactions (1) and (2), and for collisional destruction of Rydberg atoms, are measured over a wide range of n and the high-n data used to derive cross sections for free-electron capture. These cross sections are in reasonable agreement with values obtained in free-electron studies using the threshold photoelectron spectroscopy (TPSA) technique.[3] In addition, the velocity and angular distributions of the ions detected following reactions (1) and (2) were also determined. These kinematic studies show that, for both species, Br^- formation via dissociative capture is accompanied by sizable translational energy release: ~ 0.35 eV for CF_3Br; and ~ 0.2 eV for CF_2Br_2.

The present data also demonstrate that at intermediate values of n ($n \lesssim 20$), the positive and negative ions that result from Rydberg electron capture are created in sufficient proximity to each other that a significant fraction of such ion pairs possesses insufficient kinetic energy to overcome their mutual electrostatic attraction and separate, and is therefore not observed. In the case of CF_3Br, post-attachment interactions between the product ions also give rise to marked changes in the angular distribution of the detected Br^- ions. In addition, analysis of the kinematic data shows that the intermediate CF_3Br^{-*} and $CF_2Br_2^{-*}$ ions have very different lifetimes against dissociation.

EXPERIMENTAL METHOD

The experimental techniques employed in the present study are similar to those used in earlier investigations in this laboratory.[4–7] Measurements of the velocity and angular distributions of the product negative ions are used to investigate both translational energy release in dissociative capture and the effects of post-attachment interactions. Rate constants for production of free negative ions are obtained using a mixed-target-gas approach. The present apparatus is shown schematically in Fig. 1. Potassium atoms in a collimated beam are excited to a selected *nd* state by two-photon excitation using a cw Rh6G single-mode ring dye laser, the output of which is converted to a train of pulses of 1 μs duration with a pulse repetition frequency of ~ 10 kHz using a fast Pockels' cell. Excitation occurs—in zero electric field and in the presence of target gas (density $\lesssim 10^{11}$ cm^{-3})—near the center of an interaction region defined by two planar, parallel fine-mesh grids.

To measure the velocity and angular distributions of the observed product ions, collisions are allowed to occur for a predetermined time interval following excitation (typically ~ 1 μs), whereupon a small voltage pulse is applied to the lower interaction region grid to expel any collisionally produced negative ions. These ions then traverse the upper field-

 0021-9606/90/031672-05$03.00

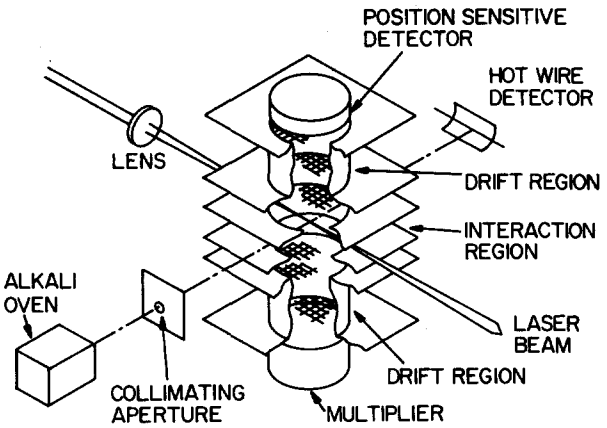

FIG. 1. Schematic diagram of the apparatus.

free drift region and, after further acceleration, are detected by a 1 in. diameter position sensitive detector (PSD). The PSD provides both the arrival time and position of each ion, and these are recorded and stored by a microcomputer. Time-of-flight techniques are used to identify the product negative ions and to distinguish ions present in the interaction region at the time of application of the extraction pulse from those formed in later collisions. The probability that a Rydberg atom is excited (and thus that an ion may be formed) during any laser pulse is small (<0.05) and product ion arrival position distributions are built up by accumulating data following many excitation pulses. These spatial distributions reflect the product of the (known) mean ion flight time and the ion velocity components in the xy (i.e., horizontal) plane. The measured spatial distributions can therefore be used to obtain both the velocity and angular distributions of the detected ions. The mean translational energy release upon dissociation, $\bar{\epsilon}_{td}$, is calculated from the negative ion spatial distributions measured at high n, where post-attachment interactions are negligible, using a procedure described in detail elsewhere.[4,5]

To obtain rate constants for free negative ion production, a mixed target gas comprising SF_6 and the target gas of interest is used. Following excitation, collisions are again allowed to occur for a predetermined time interval (typically ~ 1–$5\,\mu s$), whereupon a voltage pulse is applied to the upper interaction region grid to direct any collisionally produced negative ions into the lower field-free drift region. After traversing the drift region, the ions are accelerated to ~ 3 keV and are detected by a Johnston MM-1 electron multiplier. Time-of-flight techniques are used to separately identify product Br^- (or Br_2^-) and SF_6^- ions. Because rate constants for the formation of SF_6^- ions via the reaction

$$K(nd) + SF_6 \rightarrow K^+ + SF_6^- \qquad (3)$$

are known,[6,8] measurement of the relative SF_6^- and fragment ion signals, and relative target gas densities (measured using an ion gauge calibrated against a capacitance manometer), permit rate constants for reactions (1) and (2) to be derived. The relative detection efficiencies for the various negative ions of interest in this work could not be directly determined and are assumed to be equal. This assumption appears reasonable given that prior studies have demonstrated that, for the same impact energy, the MM-1 detection efficiencies for Cl^- and SF_6^- ions differ by only 15%.[7] Additional measurements, to be described later, also confirm the correctness of this assumption.

Use of SF_6 resulted in a small SF_5^- signal, but this signal remained even when the laser beam was blocked and is therefore not a result of Rydberg atom collisions. Use of the PSD showed that the SF_5^- ions were created along the entire length of the potassium atom beam. This, coupled with the rapid increase in SF_5^- signal observed as the potassium oven temperature (and thus relative K_2 dimer concentration in the beam) was raised, suggests their formation via the reaction

$$K_2 + SF_6 \rightarrow KF + SF_5^- + K^+. \qquad (4)$$

Rate constants k_d for destruction of Rydberg atoms in collisions with CF_2Br_2 were determined by measuring the time evolution of the *total* Rydberg atom population $N^*(t)$ in the interaction region, which is given to a good approximation by

$$N^*(t) = N^*(0)e^{-t/\tau}, \qquad (5)$$

where

$$\frac{1}{\tau} = \rho k_d + \frac{1}{\tau_{\text{eff}}} \qquad (6)$$

and $N^*(0)$ is the number of Rydberg atoms present at $t = 0$ (i.e., at the end of the laser excitation pulse), τ_{eff} is the effective parent nd state lifetime, and ρ is the target gas density. The Rydberg atom populations were determined using selective field ionization (SFI).[2,8,10] Values of $1/\tau$ were measured at several different target gas densities and k_d obtained by fitting a straight line [i.e., Eq. (6)] through the data. The rate constants for collisional destruction by CF_3Br, however, were very small and could not be reliably measured using this technique.

RESULTS AND DISCUSSION

CF_3Br

Arrival position distributions for Br^- ions detected following $K(nd)$–CF_3Br collisions are shown in Figs. 2(a) and 2(b) for $n = 40$ and $n = 10$, respectively. The distribution for $n = 40$ is circularly symmetric, indicating that the Br^- ions have an isotropic velocity distribution as is expected if electrostatic interactions between the product ions are negligible. Analysis of the data for $n = 40$, and higher n, shows that the total mean translation energy release upon dissociation $\bar{\epsilon}_{td}$ is quite large, 0.35 ± 0.05 eV, of which ~ 0.16 eV is acquired by the Br^- fragment. Indeed, as discussed elsewhere,[4] essentially all of the total available excess energy of reaction E^* (~ 0.35 eV) appears in translation. This suggests that the electron is captured directly into an antibonding orbital localized on the Br atom, whereupon immediate dissociation occurs before redistribution of the excess energy among the various vibrational modes of the intermediate CF_3Br^{-*} ion can take place. Because all the excess energy appears in translation, the distribution of released transla-

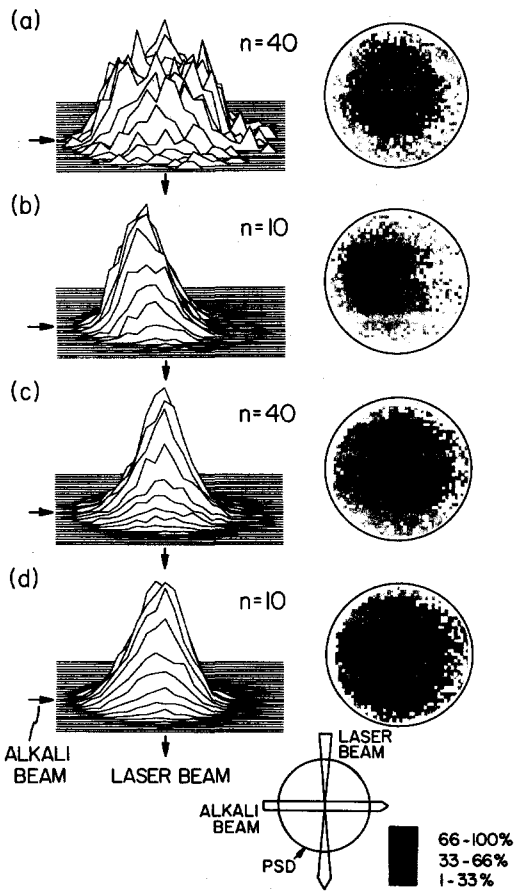

FIG. 2. Spatial distributions of Br^- ions observed following collisions of K(*nd*) Rydberg atoms with (a,b) CF_3Br and (c,d) CF_2Br_2.

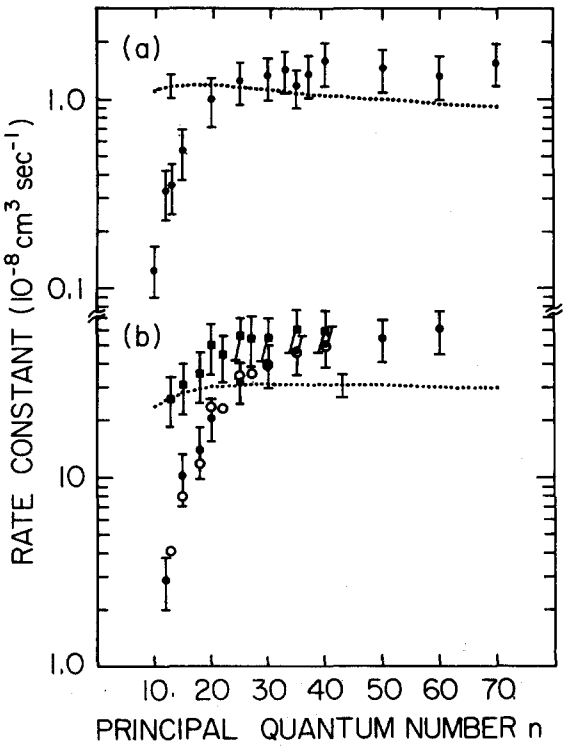

FIG. 3. Rate constants for the production of free Br^- ions (●) and for collisional destruction (■) in collisions of K(*nd*) Rydberg atoms with (a) CF_3Br and (b) CF_2Br_2. Rate constants for Rydberg electron capture obtained using free-electron cross sections measured with the TPSA technique and Eq. (7) are included (···) together with (see the text) rate constants for Br^- production derived from the product of the rate constants for collisional destruction and the computed fractional escape probabilities (○).

tional energies is expected to comprise a narrow peak centered on the mean energy $\bar{\epsilon}_{td}$ and this confirmed by detailed analysis of the form of the arrival position distribution.[4]

For values of $n \leqslant 20$, the Br^- spatial distributions become increasingly asymmetric, until at $n = 10$, the majority of the detected ions have significant velocity components antiparallel to the direction of the potassium atom beam. This striking asymmetry is a direct consequence of post-attachment interactions and of the rapid dissociation of the CF_3Br^{-*} intermediate, and may be explained qualitatively as follows. The Rydberg atoms have a thermal distribution of speeds with a mean velocity of $\sim 5.7 \times 10^4$ cm s^{-1}, which is close to the mean velocity of Br^- ions formed by dissociative capture, $\sim 6.6 \times 10^4$ cm s^{-1}. Thus, if a Br^- ion is initially created traveling in the same general direction as the K^+ core ion, their relative kinetic energy in the center-of-mass frame will be very small. In contrast, if the ions are initially oppositely directed, the relative kinetic energy will be large. As n decreases, an increasing amount of relative kinetic energy (on the order of the electron binding energy) is, on average, required to permit the ions to overcome their mutual attraction. In consequence, an increasing fraction of those ion pairs for which the Br^- ion is initially traveling in the same general direction as the K^+ core ion possess insufficient relative kinetic energy to separate and are therefore not detected, resulting in a Br^- angular distribution that is increasingly peaked in the opposite direction.

The effects of post-attachment interactions are also evident in Fig. 3(a), which shows the rate constant $k(Br^-)$ for production of free Br^- ions via reaction (1) as a function of n. The decrease in $k(Br^-)$ at the lower values of n results primarily from post-attachment interactions: ion pairs are formed but are unable to separate. For large values of n, however, post-attachment interactions are negligible and Br^- production can be discussed simply in terms of capture of the essentially free Rydberg electron by the target molecule. In this limit, the rate constant for Br^- formation should equal that for the capture of free electrons having the same velocity distribution as the Rydberg electron, i.e.,

$$k = \int_0^\infty v\sigma_e(v) f(v) dv, \tag{7}$$

where $f(v)$ is the Rydberg electron velocity distribution (determined by its quantum state) and $\sigma_e(v)$ is the cross section for capture of free electrons of velocity v. Cross sections for free electron capture to CF_3Br have been measured at low energies using the TPSA technique.[3] Rate constants calculated using these cross sections and Eq. (7) are included in Fig. 3 and are in reasonable agreement with the present data.

As is apparent from Fig. 3(a), the measured rate constants are essentially independent of n at high n, i.e., independent of the Rydberg electron velocity distribution. Inspection of Eq. (7) shows that this independence requires that $\sigma_e(v)$ be inversely proportional to electron velocity, pointing to an s-wave capture process.[11] The cross section $\sigma_e(v)$ derived from the Rydberg atom data (assuming a $1/v$ dependence) is presented in Fig. 4(a), together with velocity-averaged cross sections $\bar{\sigma}_e$ obtained by use of the relation $\bar{\sigma}_e = k(Br^-)/v_m$, where v_m is the median velocity of the attached electron, i.e., the Rydberg electron velocity such that integration of Eq. (5) from 0 to v_m yields a value one-half that for integration from 0 to ∞. The Rydberg atom data are positioned on the energy axis according to the value $1/2\, mv_m^2$. Figure 4(a) also includes the TPSA measurements, and the agreement between the Rydberg-atom and free-electron data is quite good.

CF_2Br_2

Rydberg atom collisions with CF_2Br_2 result in the formation of both Br^- and Br_2^- ions. Br^- production is, however, the dominant channel, and the ratio of the Br_2^- and Br^- signals is shown in Fig. 5 as a function of n. Br_2^- ions were also noted in earlier TPSA studies.[3]

Arrival position distributions for Br^- ions detected following $K(nd)$–CF_2Br_2 collisions are presented in Figs. 2(c) and 2(d) for $n = 40$ and 10, respectively. The distribution for $n = 40$ is circularly symmetric demonstrating that, as for CF_3Br, the product ions have an isotropic velocity distribution. Analysis of this distribution, and those obtained at higher n, shows that the mean translational energy release $\bar{\epsilon}_{td}$ is again quite large, 0.20 ± 0.03 eV, of which ~ 0.12 eV is acquired by the Br^- fragment. The shape of the spatial distribution, which is very different from that for CF_3Br, is

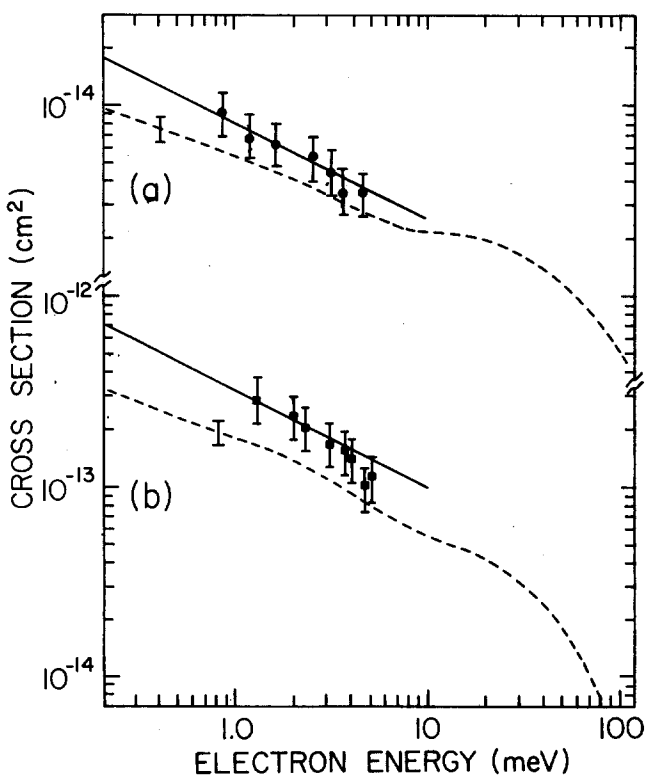

FIG. 4. Electron attachment to (a) CF_3Br and (b) CF_2Br_2. Rydberg atom data: —, $\sigma_e(v)$; ◆, ■, $\bar{\sigma}_e$. TPSA data: – –, $\sigma_e(v)$.

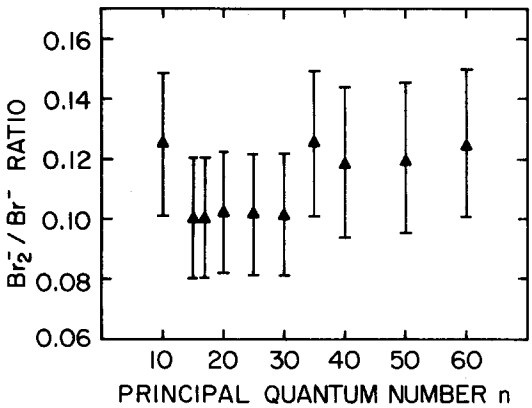

FIG. 5. Ratio of Br_2^- to Br^- production in collisions of $K(nd)$ Rydberg atoms with CF_2Br_2.

similar to that observed in earlier studies[5] of dissociative electron capture by CCl_4 and $CFCl_3$ and indicates that the Br^- ions have a broad distribution of translational energies. This, in turn, suggests that the intermediate $CF_2Br_2^{-*}$ ions must be sufficiently long lived that effective redistribution of the excess energy of reaction among internal vibrational modes can occur.

In contrast to CF_3Br, the Br^- arrival position distributions for CF_2Br_2 retain their circular symmetry at low n. This difference in behavior can be accounted for in terms of differences in the lifetimes of the intermediate $CF_2Br_2^{-*}$ and CF_3Br^{-*} ions. As discussed previously, the lifetime of the CF_3Br^{-*} intermediate is very short ($\lesssim$ a vibrational period) and dissociation occurs before the intermediate ion has moved more than a few Å. Thus, the Br^- ion is created close to the K^+ core ion and it is the post-attachment interaction between the K^+ and Br^- ions that determines the angular distribution of the Br^- ions. On the other hand, the shape of the CF_2Br_2 spatial distribution suggests that the lifetime of the $CF_2Br_2^{-*}$ intermediate is considerably longer. In this event, it is the post-attachment interaction between the K^+ and $CF_2Br_2^{-*}$ ions that is important. Those ion pairs with sufficient kinetic energy to overcome their mutual electrostatic attraction separate, following which the $CF_2Br_2^{-*}$ ions dissociate. Thus, dissociation occurs well removed from the K^+ core ion, resulting in an isotropic Br^- velocity distribtion.

This model of the interaction is supported by the observation that the ratio of the Br_2^- and Br^- signals is essentially independent of n, even at low n (see Fig. 5). Measurements of arrival position distributions for Br_2^- ions at high n showed that these ions are formed with very small translational energies ($\lesssim 0.02$ eV) and would therefore be very susceptible to post-attachment interactions. Thus, were dissociation of the $CF_2Br_2^{-*}$ ions very rapid, the different initial energies of the Br_2^- and Br^- fragments would, at low n, lead to markedly different n dependences in these signals. The near constancy of the ratio of the Br_2^- and Br^- signals therefore suggests that dissociation occurs well removed from the K^+ core ion, whereupon the Br_2^- to Br^- ratio is determined principally by the properties of the intermediate $CF_2Br_2^{-*}$ ions.

Rate constants $k(Br^-)$ for the production of free Br^- ions via reaction (2a) are presented in Fig. 3(b) and are

quite large. Also included are rate constants k_d measured for Rydberg atom destruction in collisions with CF_2Br_2. At the higher values of n, the rate constants k_d are $\sim 10\%$ to 20% higher than those for Br^- production, indicating that Br^- formation is the dominant Rydberg atom destruction mechanism. The remaining difference is associated with Br_2^- production and, possibly, collisional ionization resulting from rotational energy transfer due to the small dipole moment (~ 0.66 D) of CF_2Br_2. However, although this latter process has been observed in Rydberg atom collisions with a number of nonattaching polar targets including HF and NH_3,[12,13] SFI studies revealed very little collisional n-changing, suggesting that it is of only minor importance. The agreement between the rate constants measured for Br^- production and collisional destruction (appropriately reduced to take into account Br_2^- production) at high n indicates that no major systematic errors are inherent in assuming that Br^-, Br_2^-, and SF_6^- ions are detected with equal efficiencies by the electron multiplier.

At low n, the rate constants $k(Br^-)$ fall substantially below those for collisional destruction. This results because only a fraction of those K^+–$CF_2Br_2^{-*}$ ions pairs initially formed by Rydberg electron capture possess sufficient kinetic energy to overcome their mutual electrostatic attraction and separate. This fraction was calculated (assuming that the $CF_2Br_2^{-*}$ ions do not undergo significant dissociation during separation) as described elsewhere.[6,9] Rate constants for Br^- production obtained by multiplying the measured rate constants for collisional destruction (appropriately reduced to take into account Br_2^- production) by the calculated fractional escape probabilities are included in Fig. 3(b) and are in good agreement with the experimental observations. This agreement suggests that bound ion pairs must undergo mutual neutralization before dissociation of the $CF_2Br_2^{-*}$ intermediate can occur, a conclusion that is consistent with the kinematic data and with the n-independence of the ratio of the Br_2^- and Br^- ion signals at low n.

The rate constants for collisional destruction, however, decrease at low n. This decrease cannot be explained in terms of the velocity dependence of the free-electron attachment cross section $\sigma_e(v)$. The Rydberg electron velocity distributions encompass a broad range of velocities and there is substantial overlap between the distributions for adjacent nd states. This overlap requires that rate constants for collisional destruction vary only slowly with n, as is evident from the calculated rate constants shown in Fig. 3. The observed n dependence of k_d is believed to be a consequence of the large free-electron attachment cross section of CF_2Br_2 coupled with the finite size of the Rydberg electron "cloud." As n decreases, the electron density inside this cloud increases to the point that, for some range of heavy-particle impact parameters, the probability that a target molecule will capture the Rydberg electron during its passage through the electron cloud approaches unity. (Simple calculations indicate that, for zero-impact parameter, this condition is first encountered for $n \sim 25$.) The effect of this increasing opacity of the electron cloud is to decrease the average effective electron density seen by a target molecule, leading to a decrease in the rate constant. (In the case of CF_3Br, the free-electron attachment cross section is much smaller, and such opacity effects do not become important until much lower values of n.)

At the higher values of n, the measured rate constants for collisional destruction and for production of free Br^- ions are essentially independent of n, again pointing to s-wave capture. Rate constants for Rydberg electron capture calculated using free-electron cross sections (for Br^- production) obtained in TPSA studies[3] and Eq. (7) are included in Fig. 3(b). The cross section $\sigma_e(v)$ for Br^- production via free electron attachment derived from the collisional-destruction rate constants (again appropriately reduced to take into account Br_2^- production) are presented in Fig. 4(b). Also included are the corresponding velocity-averaged cross sections $\bar{\sigma}_e$ and the earlier TPSA results. The agreement between the Rydberg-atom and TPSA data is fair.

The present data show that studies of collisions involving atoms in high Rydberg states can provide a wealth of information regarding electron attachment processes at subthermal electron energies. In particular, such studies can be used to investigate the translational energy release that accompanies dissociative electron capture, and to set limits on the lifetimes of excited negative ion intermediates. Analyses of high-n data using the essentially free electron model yield cross sections for free electron attachment. Application of this model at low-to-intermediate values of n must be approached with caution, however, because post-attachment interactions between the product ion pairs become important, even in cases where the product negative ions are formed with appreciable kinetic energies.

ACKNOWLEDGMENTS

This research is supported by the National Science Foundation under Grant No. PHY87-09637 and by the Robert A. Welch Foundation.

[1]For a discussion of this model see, for example, the articles by M. Matsuzawa and by A. P. Hickman, R. E. Olson, and J. Pascale, in *Rydberg States of Atoms and Molecules*, edited by R. F. Stebbings and F. B. Dunning (Cambridge University, New York, 1983).
[2]F. B. Dunning, J. Phys. Chem. **91**, 2244 (1987).
[3]S. H. Alajajian, M. T. Bernius, and A. Chutjian, J. Phys. B **21**, 4021 (1988).
[4]C. W. Walter, B. G. Lindsay, K. A. Smith, and F. B. Dunning, Chem. Phys. Lett. **154**, 409 (1989).
[5]C. W. Walter, K. A. Smith, and F. B. Dunning, J. Chem. Phys. **90**, 1652 (1989).
[6]Z. Zheng, K. A. Smith, and F. B. Dunning, J. Chem. Phys. **89**, 6295 (1988).
[7]R. W. Marawar, C. W. Walter, K. A. Smith, and F. B. Dunning, J. Chem. Phys. **88**, 176 (1988).
[8]B. G. Zollars, C. Higgs, F. Lu, C. W. Walter, L. G. Gray, K. A. Smith, F. B. Dunning, and R. F. Stebbings, Phys. Rev. A **32**, 3330 (1985).
[9]B. G. Zollars, C. W. Walter, F. Lu, C. B. Johnson, K. A. Smith, and F. B. Dunning, J. Chem. Phys. **84**, 5589 (1986).
[10]See, for example, F. G. Kellert, T. H. Jeys, G. B. McMillian, K. A. Smith, F. B. Dunning, and R. F. Stebbings, Phys. Rev. A **23**, 1127 (1981).
[11]A. Chutjian and S. H. Alajajian, Phys. Rev. A **31**, 2885 (1985).
[12]A. Kalamarides, L. N. Goeller, K. A. Smith, F. B. Dunning, M. Kimura, and N. F. Lane, Phys. Rev. A **36**, 3108 (1987).
[13]F. G. Kellert, K. A. Smith, R. D. Rundel, F. B. Dunning, and R. F. Stebbings, J. Chem. Phys. **72**, 3179 (1980).